for pressure. Subscripts, c and s, means UMI simulation or ordinary simulation and the standard solution, respectively.

3.2. *Results and discussion*

The results of the UMI simulation with/without pressure compensation were evaluated by error norms of the velocity vector and pressure in feedback domain M (or the aneurysmal domain), $\bar{e}_{\mathrm{M}}(\mathbf{u},\ t)$ and $\bar{e}_{\mathrm{M}}(p,\ t)$, and compared with those of the ordinary numerical simulation. The variations of $\bar{e}_{\mathrm{M}}(\mathbf{u},\ t)$ and $\bar{e}_{\mathrm{M}}(p,\ t)$ of the UMI simulations at $K_{\mathrm{v}}^{*} = 0$, 80 and 160 are shown in Figure 3. The UMI simulations diverge at $K_{\mathrm{v}}^{*} \geqslant 170$ in the case of $\Delta t = 0.01$ as revealed in our previous study [22]. There is an inversely proportional relationship between the time increment and the maximum feedback gain. Concerning this issue, we theoretically clarified that the feedback signal in the source term destabilized the iterative calculation, and proposed a computational scheme to remove the destabilization phenomenon [32]. However, we used the previous scheme in this study because improvement of computational accuracy of pressure can be discussed in a stable region with the feedback gain of $K_{\mathrm{v}}^{*} < 170$. In the case of $K_{\mathrm{v}}^{*} = 0$, which corresponds to the ordinary simulation without feedback, neither error norm temporally changes because the steady solution was set as the initial condition (a dotted line in Figure 3). In contrast, by applying feedback in the UMI simulations at $K_{\mathrm{v}}^{*} = 80$ and 160, the error norm of the velocity vector, $\bar{e}_{\mathrm{M}}(\mathbf{u},\ t)$, monotonically decreases and converges at each constant value (dashed and solid black lines in Figure 3(a)). This indicates that the velocity field of the UMI simulation is closer to the standard solution than that of the ordinary

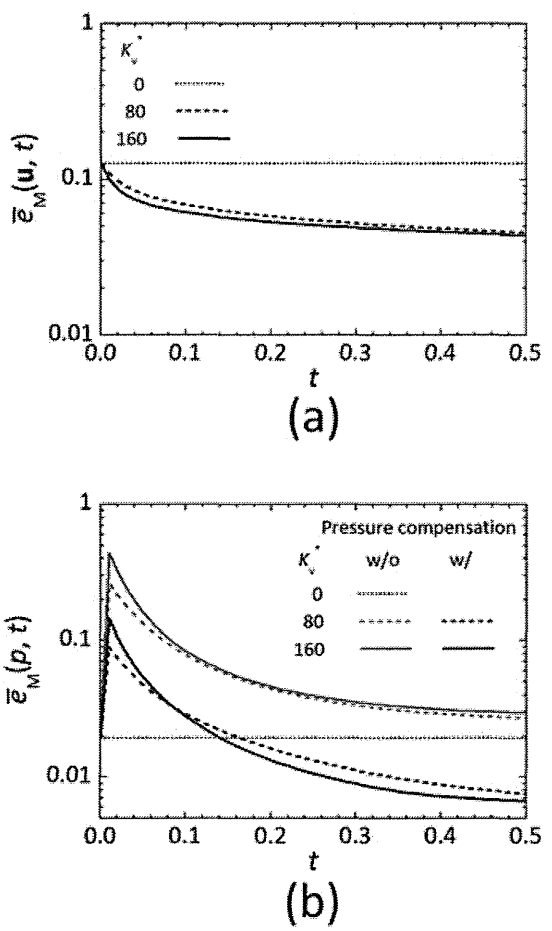

Figure 3. Transient changes of space-averaged error norms of (a) velocity vector and (b) pressure in the feedback domain in the UMI simulations without/with pressure compensation at $K_{\mathrm{v}}^{*} = 0$, 80, and 160 (nondimensional).

DOI: 10.1002/cnm

simulation. Moreover, the larger feedback gain reduces the error more rapidly. On the other hand, the error norm of pressure, $\bar{e}_M(p,\ t)$, of the UMI simulations without pressure compensation drastically increases at the first time step ($t = 0.01$), and then decreases toward each constant value (dashed and solid gray lines in Figure 3(b)). With either feedback gain, the convergent value of $\bar{e}_M(p,\ t)$ remains larger than that of the ordinary simulation, indicating deterioration of the computational accuracy of the pressure field by the feedback. Generally, improvement of the computational accuracy of the velocity field leads to better reproduction of the pressure field as time progresses. However, as described in the theoretical analysis, pressure error against the standard solution arises because the feedback signals do not become zero so as to reduce the error derived from a constant difference of the boundary conditions. The results of $\bar{e}_M(p,\ t)$ by the UMI simulations at $K_v^* = 80$ and 160 with pressure compensation are presented with dashed and solid black lines in Figure 3(b), respectively. In the time of $t > 0.2$, the error norms of the pressure of the UMI simulations are smaller than that of the ordinary simulation. This means that the pressure field approaches the standard solution, cancelling the error in the pressure field caused by feedback signals. Moreover, the UMI simulation with a large feedback gain $\left(K_v^* = 160\right)$ presents a larger value of $\bar{e}_M(p,\ t)$ than that of the UMI simulation with a small feedback gain $\left(K_v^* = 80\right)$ at the beginning of the computation, but it finally gives a smaller convergent value.

The variations of steady values of the space-averaged error norms of the velocity vector and pressure in the feedback domain M, $\bar{e}_M(\mathbf{u},\ t_\infty)$ and $\bar{e}_M(p,\ t_\infty)$ ($t_\infty = 20$), with the feedback gain are shown in Figure 4. In the UMI simulation, the value of $\bar{e}_M(\mathbf{u},\ t_\infty)$ monotonically decreases

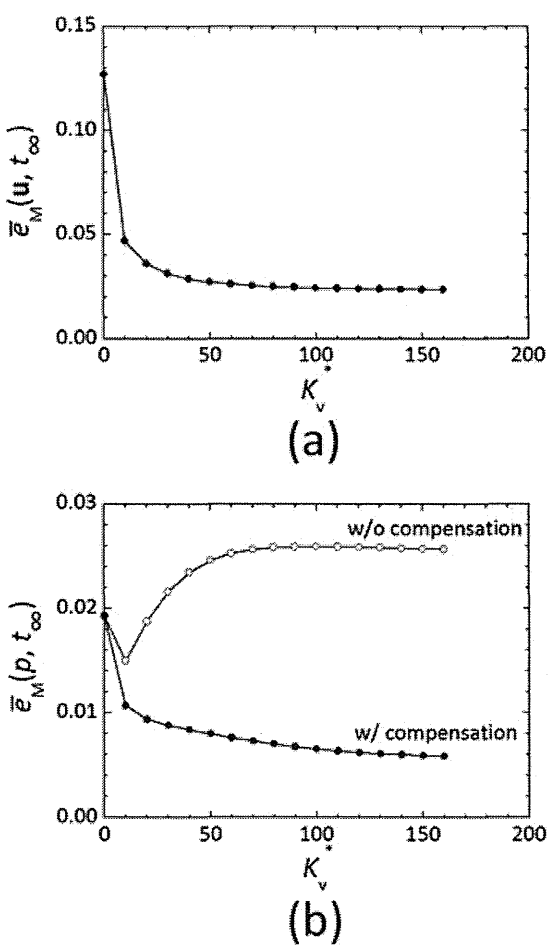

Figure 4. Variations of steady values of space-averaged error norms of (a) velocity vector and (b) pressure in the feedback domain with feedback gain (nondimensional).

DOI: 10.1002/cnm

with increasing feedback gain (Figure 4(a)). Note that the error norm of the velocity vector in the UMI simulation is not affected by the pressure compensation. However, the value of $\bar{e}_{\mathrm{M}}(p,\ t_\infty)$ at first decreases and then increases (open circle plots in Figure 4(b)). In $K_{\mathrm{v}}^* > 20$, the error norm is larger than that of the ordinary simulation $\left(K_{\mathrm{v}}^* = 0\right)$. When the feedback gain is relatively small $\left(K_{\mathrm{v}}^* < 20\right)$, the computational accuracy of the pressure field seems to be improved in accordance with the improvement of that of the velocity field because the pressure deviation as a result of the application of artificial body forces (or feedback signals) is not significant. With large feedback gain, however, the ability to reproduce the pressure field deteriorates because the significant artificial body forces proportional to the feedback gain are applied. In contrast, as the feedback gain increases, the value of $\bar{e}_{\mathrm{M}}(p,\ t_\infty)$ after the pressure compensation monotonically decreases, similar to that of the velocity vectors (solid circle plots in Figure 4(b)). This reflects the fact that the pressure field concurrently becomes closer to the standard solution with the velocity field. Regarding the determination of the feedback gain, K_{v}^*, in the practical application of the UMI simulation, although the UMI simulation with a large feedback gain reduces the error against the measurement data, it reproduces the measurement error as well. In our previous study [23], the effects of major measurement errors on the computational accuracy of the UMI simulation were investigated, and methods to compensate those effects were proposed. An appropriate value of the feedback gain should be determined based on the results, considering how much compensation is achieved. It is also noted that the UMI simulation has sufficiently high frequency response characteristics to ensure the convergence to the unsteady flow [22].

The result of the UMI simulation at $K_{\mathrm{v}}^* = 160$ is further investigated in the following. The steady values of the space-averaged error norms of velocity vector and pressure against the standard solution in each z-directional cross-section, $\bar{e}_{\mathrm{cs}(z)}(\mathbf{u},\ t_\infty)$ and $\bar{e}_{\mathrm{cs}(z)}(p,\ t_\infty)$ ($t_\infty = 20$), in the ordinary simulation $\left(K_{\mathrm{v}}^* = 0\right)$ and the UMI simulations without/with the pressure compensation are shown in Figure 5(a) and (b), respectively. The dotted line and the gray and black solid lines represent the results of the ordinary simulation and the UMI simulations without and with the pressure compensation, respectively, and the gray area indicates the feedback domain in the UMI simulation. Compared with the ordinary simulation, in the case of the UMI simulations, the error norm of the velocity vector, $\bar{e}_{\mathrm{cs}(z)}(\mathbf{u},\ t_\infty)$, is decreased after the feedback domain ($z \geq 1.193$), and remains smaller in a certain downstream region of the feedback domain ($2.897 < z < 3.8$), as shown by the solid lines in Figure 5(a). Regarding the error norm of pressure, $\bar{e}_{\mathrm{cs}(z)}(p,\ t_\infty)$, shown in Figure 5(b), the UMI simulation with the pressure compensation presented a smaller value than the ordinary simulation in all z-directional cross-sections and almost the same value near the downstream boundary, implying the ability to reproduce the pressure field with good accuracy. On the other hand, the error norm of pressure, $\bar{e}_{\mathrm{cs}(z)}(p,\ t_\infty)$, in the UMI simulation without pressure compensation increases in the upstream region of the feedback domain and exceeds that of the ordinary simulation with the peak value near the upstream boundary of the feedback domain. It then decreases in the downstream direction and becomes the same as that in the UMI simulation with the pressure compensation. Figure 5(c) shows a summation of absolute values of the divergence of the feedback force vector in each z-directional cross-section. The value is large in the upstream side in the feedback domain where the error in the velocity field is large, especially at the upstream boundary of the feedback domain where feedback signals discontinuously change. Moreover, in comparison with Figure 5(b), the large value of the divergence of the feedback force vector also influences the computational accuracy of the pressure field in the upstream domain before the feedback domain where the divergence is zero.

The pressure distributions on a y-directional cross-section ($y = 1.462$) of the standard solution, the ordinary simulation $\left(K_{\mathrm{v}}^* = 0\right)$, and the UMI simulations $\left(K_{\mathrm{v}}^* = 160\right)$ without/with the pressure compensation are depicted in Figure 6. Between the pressure fields of the standard solution and the ordinary simulation, p_{s} and p_{o} (Figures 6(a) and (b)), a difference can be observed near the upstream boundary, but similar pressure profiles are obtained in the aneurysm. As observed in the error norm of pressure in Figure 5(b), the UMI simulation without pressure compensation (Figure 6(c)) provides a pressure distribution different from that of the standard solution (Figure 6(a)), especially in the upstream region of the feedback domain (see an arrow), but it gives almost the same distribution in the aneurysm. In the UMI simulation with the pressure compensation (Figure 6(d)),

DOI: 10.1002/cnm

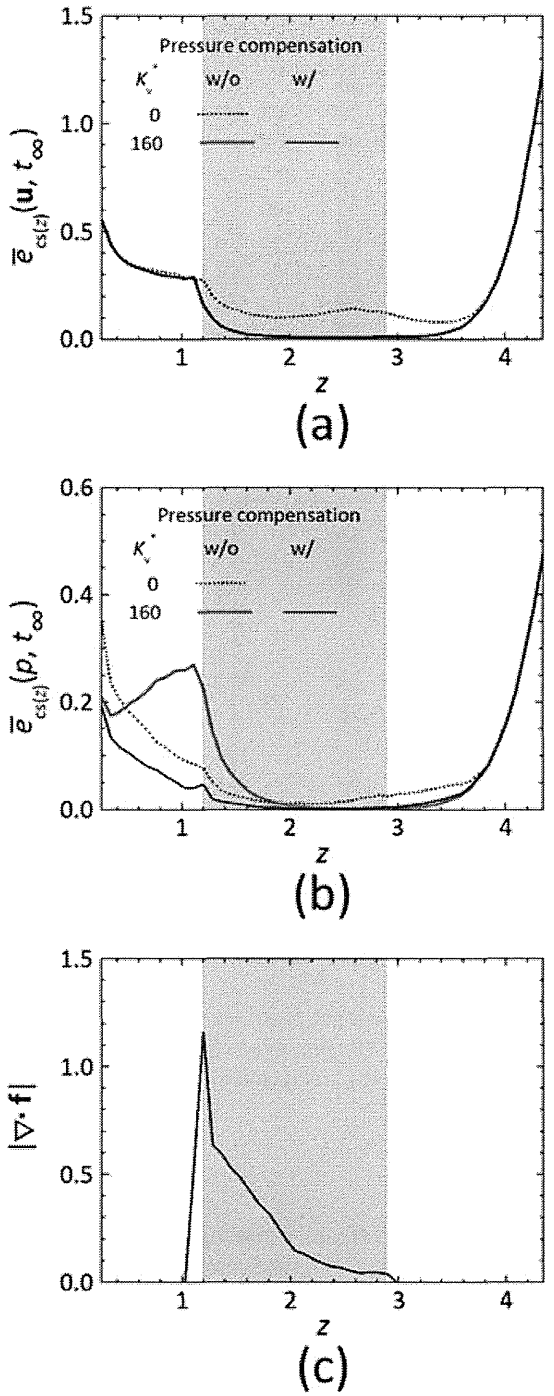

Figure 5. Steady values of space-averaged error norms of (a) velocity vector and (b) pressure, and (c) space-averaged absolute value of divergence of feedback signal vector in each z-directional cross-section (nondimensional). The gray zone implies the feedback domain.

the difference in pressure distribution observed in the UMI simulation without the pressure compensation is properly improved.

The distributions of error norm of pressure against the standard solution on the corresponding y-directional cross-section are shown in Figure 7. As mentioned above, the ordinary simulation and the UMI simulation without the pressure compensation show relatively large error near the upstream

DOI: 10.1002/cnm

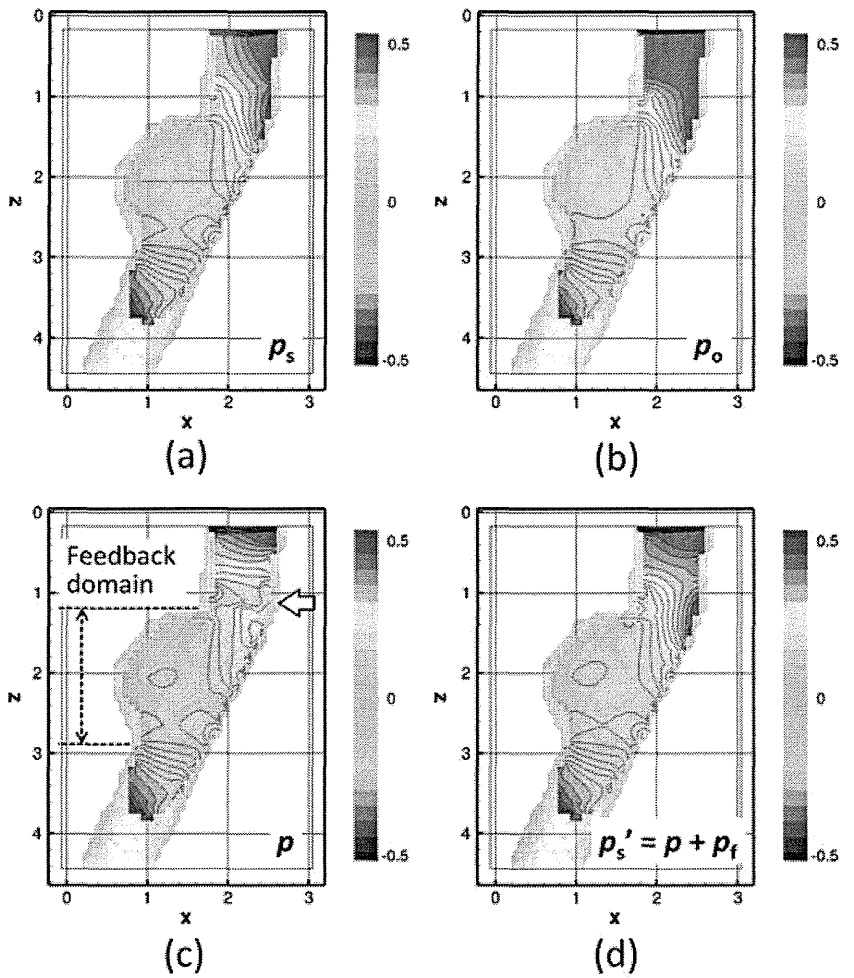

Figure 6. Pressure distribution on a y-directional cross-section ($y = 1.462$): (a) standard solution, p_s, (b) ordinary simulation $\left(K_v^* = 0\right)$, p_o, and UMI simulations (c) without and (d) with pressure compensation at $K_v^* = 160$, p and p_s', respectively (nondimensional).

boundary and in the vicinity of the upstream boundary of the feedback domain, respectively. In contrast, the error in the UMI simulation with the pressure compensation is relatively small in the whole domain.

The distribution of the divergence of the feedback force vector in the UMI simulation is demonstrated in Figure 8(a). There is a region with a large magnitude of divergence of the feedback force vector near the upstream boundary of the feedback domain. Figure 8(b) shows the distribution of the pressure compensation in the UMI simulation, p_f, calculated from Equation (9). It is noted that the distribution of the pressure compensation has a pattern similar to that of the error norm of the pressure for the UMI simulation without the pressure compensation in Figure 7(b). By adding the pressure compensation, p_f (Figure 8(b)), to the result of the UMI simulation without compensation (Figure 6(c)), a compensated pressure field, p_s' (Figure 6(d)), is obtained.

In summary, the numerical experiment dealing with a three-dimensional steady flow in a thoracic aneurysm indicates that feedback signals in the UMI simulation can deteriorate the reproducibility of the pressure field, while improving that of the velocity field. However, by properly compensating the effects of the feedback signals on the pressure with the proposed method, both the velocity and pressure fields of the standard solution can be properly reproduced.

DOI: 10.1002/cnm

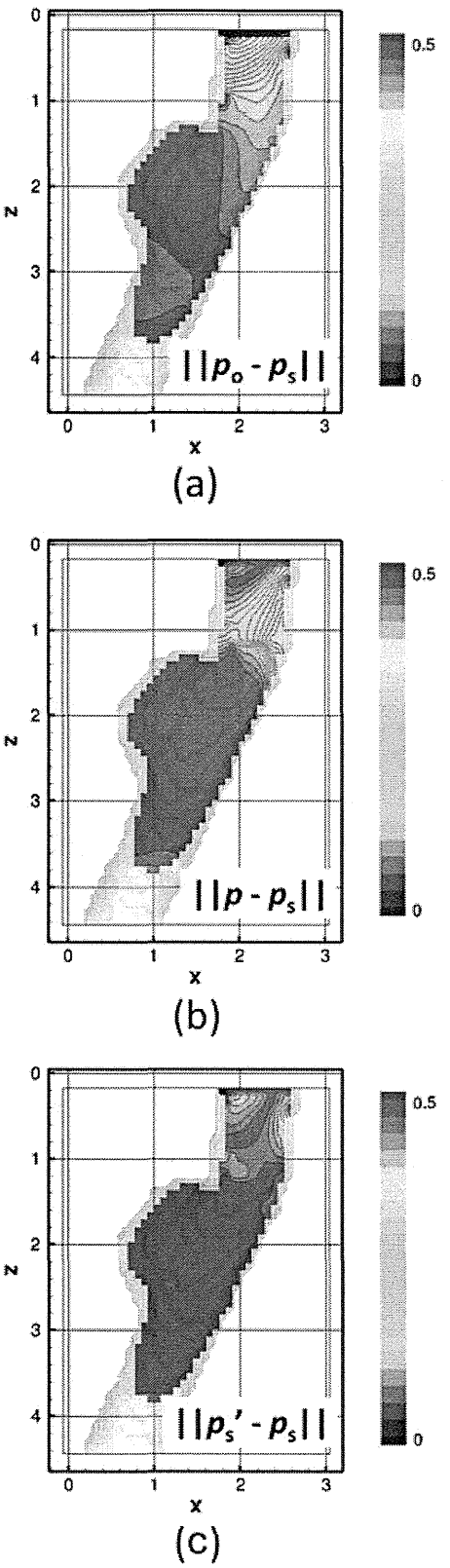

Figure 7. Error norm of pressure on a y-directional cross-section ($y = 1.462$): (a) ordinary numerical simulation $\left(K_v^* = 0\right)$, and UMI simulations (b) without and (c) with pressure compensation at $K_v^* = 160$, respectively (nondimensional).

DOI: 10.1002/cnm

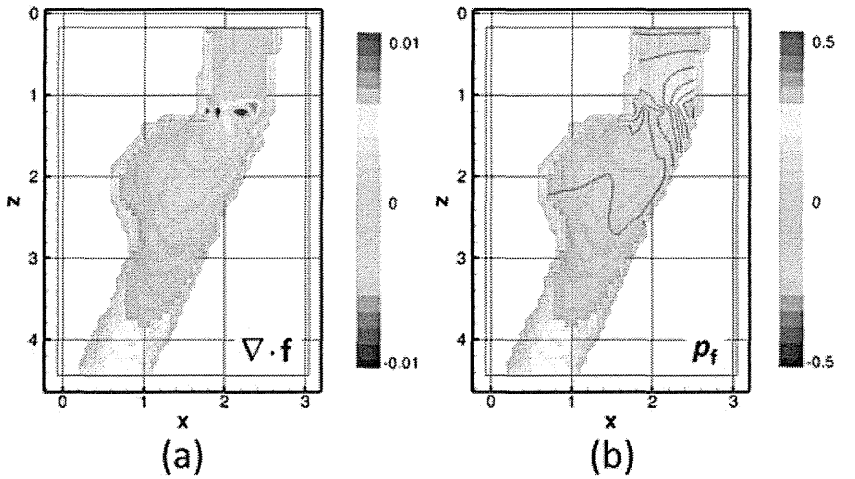

Figure 8. Distributions of (a) divergence of feedback force vector and (b) value for pressure compensation, p_f, in the UMI simulation at $K_v^* = 160$ (nondimensional).

4. CONCLUSION

In this study, reproduction of the pressure field by UMI simulation was investigated. The effect of feedback based on Doppler velocity on the pressure field was first examined by theoretical analysis. When the divergence of the feedback force vector was not zero, it influenced the pressure field in the UMI simulation, while improving the computational accuracy of the velocity field. Hence, a method to estimate the correct pressure by compensating the pressure field was devised. A numerical experiment was conducted dealing with the reproduction of a three-dimensional steady flow in a thoracic aneurysm to validate results of the theoretical analysis. The ability of the UMI simulation to reproduce the pressure field deteriorated with a large feedback gain. However, by properly compensating the effects of the feedback signals on the pressure, the error in the pressure field was reduced, exhibiting improvement of the computational accuracy in comparison with that of the ordinary simulation. Hence, the UMI simulation with pressure compensation allows for the reproduction of both velocity and pressure fields of blood flow. The information on hemodynamic stresses (wall shear stress and pressure) and blood flow dynamics enables a better understanding of blood flow and would provide novel indices for diagnosis of diseases. To perform the UMI simulation in a clinical setting, further investigations on automatic excursion of the sequential computation including reconstruction of the blood vessel configuration and recognitions of the position and orientation of the ultrasound probe are required.

REFERENCES

1. Friedman MH, Krams R, Chandran KB. Flow interactions with cells and tissues: cardiovascular flows and fluid-structure interactions. *Annals of Biomedical Engineering* 2010; **38**:1178–1187.
2. Taylor CA, Steinman DA. Image-based modeling of blood flow and vessel wall dynamics: applications, methods and future directions. *Annals of Biomedical Engineering* 2010; **38**:1188–1203.
3. Morris L, Delassus P, Grace P, Wallis F, Walsh M, McGloughlin T. Effects of flat, parabolic and realistic steady flow inlet profiles on idealised and realistic stent graft fits through Abdominal Aortic Aneurysms (AAA). *Medical Engineering & Physics* 2006; **28**:19–26.
4. Moyle KR, Antiga L, Steinman DA. Inlet conditions for image-based CFD models of the carotid bifurcation: is it reasonable to assume fully developed flow? *Journal of Biomechanical Engineering-Transactions of the ASME* 2006; **128**:371–379.
5. Formaggia L, Gerbeau JF, Nobile F, Quarteroni A. Numerical treatment of defective boundary conditions for the Navier-Stokes equations. *SIAM Journal on Numerical Analysis* 2002; **40**:376–401.
6. Veneziani A, Vergara C. An approximate method for solving incompressible Navier-Stokes problems with flow rate conditions. *Computer Methods in Applied Mechanics and Engineering* 2007; **196**:1685–1700.

DOI: 10.1002/cnm

7. McGregor RH, Szczerba D, von Siebenthal M, Muralidhar K, Szekely G. Exploring the use of proper orthogonal decomposition for enhancing blood flow images via computational fluid dynamics. *Medical Image Computing and Computer Assisted Intervention* 2008; **11**:782–789.
8. McGregor RH, Szczerbal D, Muralidhar K, Szekely G. A fast alternative to computational fluid dynamics for high quality imaging of blood flow. *Medical Image Computing and Computer Assisted Intervention* 2009; **12**:124–131.
9. Zeldin BA, Meade AJ. Integrating experimental data and mathematical models in simulation of physical systems. *AIAA Journal* 1997; **35**:1787–1790.
10. Dwight RP. Bayesian inference for data assimilation using least-squares finite element methods. *IOP Conference Series: Materials Science and Engineering* 2010; **10**:012224.
11. Heys JJ, Manteuffel TA, McCormick SF, Milano M, Westerdale J, Belohlavek M. Weighted least-squares finite elements based on particle imaging velocimetry data. *Journal of Computational Physics* 2010; **229**:107–118.
12. Bertoglio C, Moireau P, Gerbeau JF. Sequential parameter estimation for fluid-structure problems. Application to hemodynamics. *International Journal for Numerical Methods in Biomedical Engineering* 2012; **28**:434–455.
13. D'Elia M, Perego M, Veneziani A. A variational data assimilation procedure for the incompressible Navier-Stokes equations in hemodynamics. *Journal of Scientific Computing* 2012; **52**:340–359.
14. Munro R, Kopken C, Kelly G, Thepaut JN, Saunders R. Assimilation of Meteosat radiance data within the 4D-Var system at ECMWF: data quality monitoring, bias correction and single-cycle experiments. *Quarterly Journal of the Royal Meteorological Society* 2004; **130**:2293–2313.
15. Hayase T, Hayashi S. State estimator of flow as an integrated computational method with the feedback of online experimental measurement. *Journal of Fluids Engineering-Transactions of the ASME* 1997; **119**:814–822.
16. Nisugi K, Hayase T, Shirai A. Fundamental study of hybrid wind tunnel integrating numerical simulation and experiment in analysis of flow field. *JSME International Journal Series B-Fluids and Thermal Engineering* 2004; **47**:593–604.
17. Yamagata T, Hayase T, Higuchi H. Effect of feedback data rate in PIV measurement-integrated simulation. *Journal of Fluid Science and Technology* 2008; **3**:477–487.
18. Nakao M, Kawashima K, Kagawa T. Application of MI simulation using a turbulent model for unsteady orifice flow. *Journal of Fluids Engineering-Transactions of the ASME* 2009; **131**:111401.
19. Funamoto K, Hayase T, Shirai A, Saijo Y, Yambe T. Fundamental study of ultrasonic-measurement-integrated simulation of real blood flow in the aorta. *Annals of Biomedical Engineering* 2005; **33**:415–428.
20. Funamoto K, Suzuki Y, Hayase T, Kosugi T, Isoda H. Numerical validation of MR-measurement-integrated simulation of blood flow in a cerebral aneurysm. *Annals of Biomedical Engineering* 2009; **37**:1105–1116.
21. Funamoto K, Hayase T, Saijo Y, Yambe T. Numerical experiment for ultrasonic-measurement-integrated simulation of three-dimensional unsteady blood flow. *Annals of Biomedical Engineering* 2008; **36**:1383–1397.
22. Funamoto K, Hayase T, Saijo Y, Yambe T. Numerical experiment of transient and steady characteristics of ultrasonic-measurement-integrated simulation in three-dimensional blood flow analysis. *Annals of Biomedical Engineering* 2009; **37**:34–49.
23. Funamoto K, Hayase T, Saijo Y, Yambe T. Numerical analysis of effects of measurement errors on ultrasonic-measurement-integrated simulation. *IEEE Transactions on Biomedical Engineering* 2011; **58**:653–663.
24. Funamoto K, Hayase T, Saijo Y, Yambe T. Numerical study on variation of feedback methods in ultrasonic-measurement-integrated simulation of blood flow in the aneurysmal aorta. *JSME International Journal Series C-Mechanical Systems, Machine Elements and Manufacturing* 2006; **49**:144–155.
25. Arfken GB, Weber HJ. *Mathematical Methods for Physicists*. Elsevier Academic Press: Amsterdam/Boston/Tokyo, 2005.
26. Patankar SV. *Numerical Heat Transfer and Fluid Flow*. Hemisphere Pub. Corp.: Washington DC/New York, 1980.
27. Morbiducci U, Ponzini R, Rizzo G, Biancolini ME, Iannaccone F, Gallo D, Redaelli A. Synthetic dataset generation for the analysis and the evaluation of image-based hemodynamics of the human aorta. *Medical & Biological Engineering & Computing* 2012; **50**:145–154.
28. Swillens A, De Schryver T, Lovstakken L, Torp H, Segers P. Assessment of numerical simulation strategies for ultrasonic color blood flow imaging, based on a computer and experimental model of the carotid artery. *Annals of Biomedical Engineering* 2009; **37**:2188–2199.
29. Hayase T, Humphrey JAC, Greif R. Mini-manual for ROTFLO2. *Department of Mechanical Engineering Report*, University of California, Berkeley, 1990; FM-90-1.
30. Hayase T, Humphrey JAC, Greif R. A consistently formulated QUICK scheme for fast and stable convergence using finite-volume iterative calculation procedures. *Journal of Computational Physics* 1992; **98**:108–118.
31. Schneider GE, Zedan M. A modified strongly implicit procedure for the numerical solution of field problems. *Numerical Heat Transfer* 1981; **4**:1–19.
32. Hayase T, Imagawa K, Funamoto K, Shirai A. Stabilization of measurement-integrated simulation by elucidation of destabilizing mechanism. *Journal of Fluid Science and Technology* 2010; **5**:632–647.

DOI: 10.1002/cnm

電気学会論文誌 C（電子・情報・システム部門誌）
IEEJ Transactions on Electronics, Information and Systems
Vol.132 No.12 pp.1943–1948　DOI: 10.1541/ieejeiss.132.1943

論　文

植込み型除細動器への実装を考慮した致死性不整脈検出アルゴリズムの改良

正　員　阿部　　誠*　非会員　吉澤　　誠**　非会員　テルマ　ケイコ　スガイ***
非会員　本間　経康**　非会員　杉田　典大*　非会員　清水　一夫****
非会員　後藤　　萌****　非会員　稲垣　正司*5　非会員　杉町　　勝*5
非会員　砂川　賢二*6

Improving Detection Algorithm of Life-threatening Arrhythmias for Implementation of Implantable Cardioverter-Defibrillators

Makoto Abe*, Member, Makoto Yoshizawa**, Non-member, Telma Keiko Sugai***, Non-member, Noriyasu Homma**, Non-member, Norihiro Sugita*, Non-member, Kazuo Shimizu****, Non-member, Moe Goto****, Non-member, Masashi Inagaki*5, Non-member, Masaru Sugimachi*5, Non-member, Kenji Sunagawa*6, Non-member

（2012年2月29日受付，2012年6月28日再受付）

The implantable cardioverter-defibrillator (ICD) is an effective therapeutic device for rescuing patients with cardiac diseases from death caused by life-threatening arrhythmias. The authors previously proposed a detection algorithm of life-threatening arrhythmias with a multiple regression model. To enhance the classification accuracy, in the present study, we have introduced an autoregressive filter and a multiple detection process into the previous detection algorithm. The experimental results showed that the proposed method could attain a high accuracy such that all ventricular fibrillation rhythms could be exactly detected. In addition, detection errors of sinus rhythms or supraventricular tachyarrhythmias provoking the ICD malfunction were reduced.

キーワード：植込み型除細動器，致死性不整脈，重回帰モデル
Keywords: implantable cardioverter-defibrillator, life-threatening arrhythmia, multiple regression model

1. はじめに

日本における心血管系疾患に起因する心臓突然死による年間死者数は6万人以上といわれており，その対策は医学的かつ社会的な課題となっている[1]。心臓突然死において心臓が停止する直接の原因は，心室頻拍 (VT: Ventricular Tachycardia) や心室細動 (VF: Ventricular Fibrillation) といわれる心室性頻脈性不整脈であり，全体の80～90%を

* 東北大学大学院工学研究科
〒980-8578　宮城県仙台市青葉区荒巻字青葉6-3
Graduate School of Engineering, Tohoku University
6-3, Aoba, Aoba-ku, Sendai, Miyagi 980-8578, Japan
** 東北大学サイバーサイエンスセンター
〒980-8578　宮城県仙台市青葉区荒巻字青葉6-3
Cyberscience Center, Tohoku University
6-3, Aoba, Aoba-ku, Sendai, Miyagi 980-8578, Japan
*** 東北大学大学院医工学研究科
〒980-8578　宮城県仙台市青葉区荒巻字青葉6-3
Graduate School of Biomedical Engineering, Tohoku University
6-3, Aoba, Aoba-ku, Sendai, Miyagi 980-8578, Japan
**** オリンパス (株)
〒192-8512　東京都八王子市久保山町2-3
Olympus Corporation
2-3, Kuboyama-cho, Hachioji, Tokyo 192-8512, Japan
*5 国立循環器病研究センター研究所
〒565-8565　大阪府吹田市藤白台5-7-1
National Cerebral and Cardiovascular Center Research Institute
5-7-1, Fujishirodai, Suita, Osaka 565-8565, Japan
*6 九州大学大学院医学研究院
〒812-8582　福岡県福岡市東区馬出3-1-1
Graduate School of Medicine, Kyushu University
3-1-1, Maidashi, Higashi-ku, Fukuoka, Fukuoka 812-8582, Japan

占める[2][3]。これらの致死性不整脈は，心疾患を抱えている患者のみならず，健康な子どもや成人のスポーツ選手であっても突如として発症することがある。そこで，近年では，自動体外式除細動器 (AED: Automated External Defibrillator) が学校や公共施設に設置され，その普及によって発症後の救命率が上がっている。一方，このような致死性不整脈は再発率が高いと言われており，致死性不整脈発作を起こした患者の再発後の早期治療システムが必要である。そこで，1960 年代に Mirowski らにより植込み型除細動器 (ICD: Implantable Cardioverter Defibrillator) と呼ばれる装置が提唱され，実用化に至っている[4]。

現在は，洞性頻拍および上室性不整脈 (SVT: supraventricular tachyarrhythmia) などの致死性でない不整脈に対する誤作動を防ぐため，心房内電位もモニタすることで致死性不整脈の鑑別をより確実に行う第 5 世代 ICD が臨床使用されている[5]。しかし，既存の ICD における不整脈検出アルゴリズムでは，主として心電図 (ECG: electrocardiogram) の時間間隔情報に基づいて VF や VT の発生検出を行っているものがほとんどであるため，VF と VT を確実に区別することが困難である。また，一方で ICD が致死的ではない不整脈を誤認して不適切な治療が行われることがあり[6]~[8]，致死性不整脈を的確に検出する ICD の開発が急務とされている。

従来の方法に対し，われわれの研究グループでは，複数の心内心電図信号 (IECG: Intracardiac electrocardiogram) から複数の指標を求め，それらを説明変数とし，不整脈の種類を目的変数とする重回帰モデルを用いる方法を提案し，高精度かつ早期の不整脈検出が可能であることを示してきた[9][10]。この提案方法によって，R-R 間隔以外の情報も用いることで，不整脈をより柔軟に特徴づけることが可能となっている。しかし，それらの研究では，モデルへの入力として用いたデータに含まれる不整脈 (SVT, VT, VF) の割合が，正常洞調律 (SR: sinus rhythm) の割合に比べてかなり少なく，このことが誤検出の原因となっていた。そのため，VF の不検出率を 0 に近づけることが難しく，臨床応用上問題となる可能性があった。

そこで，本研究では，不整脈の割合が SR に比べて小さいデータ群において，誤検出の少ない重回帰モデルの作成方法を提案する。さらに，先行研究[10]の方法をさらに発展させることで，VF の不検出率を 0 に近づけるとともに，ICD の誤作動の原因となる誤検出をできるだけ減らすことを目的とする。

2. 方　法

〈2·1〉 実験データとその処理　本研究では，先行研究[9][10]と同様に，5 頭の成犬を対象とした急性実験のデータを用いた。データは，左心室内 ($IECG_{LV}$)，右心室内 ($IECG_{RV}$)，および右心房内 ($IECG_{RA}$) において取得した心内心電図であり，250 Hz にて再サンプリングを行ったものを用いた。なお，不整脈の自然発生を計測するのは困難であるため，電気刺激によって Fig.1 のように SVT, VT および VF を模擬した。なお，データには 1 度だけ自然発生した VF も含まれている。

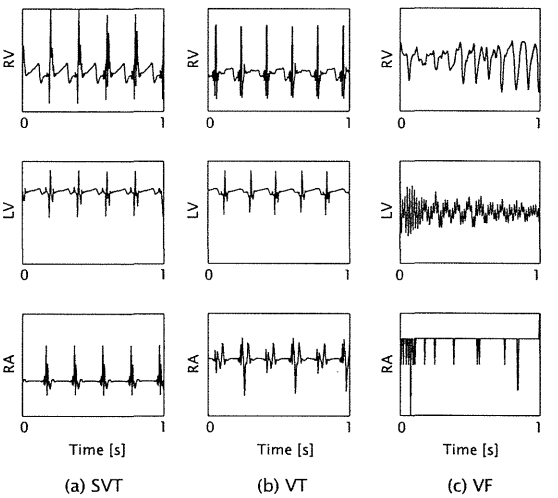

Fig. 1. Examples of IECG signals of (a) SVT, (b) VT, and (c) VF

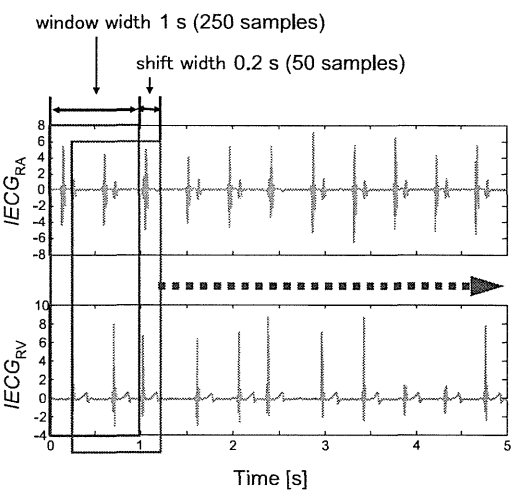

Fig. 2. Data acquisition using a 1 s long window shifting every 0.2 s

最初に，取得した心内心電図データに対して，0.8 Hz~40 Hz の帯域通過型フィルタを用いてノイズ成分を除去した。フィルタ処理後，Fig.2 に示すように，1 s の長さの窓を用いて 0.2 s ずつシフトさせながらデータを抽出した。本研究では，窓ごとに心内心電図の特徴量に基づく指標を算出した。ここで，それぞれの心調律における窓の個数を Table 1 に示す。Table 1 からわかるように，SR が約 67% を占め，その他の心調律の割合が低い。それゆえ，重回帰モデルの推定方法を工夫しないと SR の検出に特化したモデルとなってしまう可能性がある。

(倫理面への配慮)

実験に用いた成犬は，国立循環器病研究センター研究所の倫理委員会の規定に従って適切に管理され，実験は苦痛を与えない麻酔下で行われた。

Table 1. Number of windows and total duration of the data of each rhythm

	Number of windows	Duration [s]	Rate [%]
SR	3509	728.2	67.3
SVT	284	61.6	5.4
VT	474	102	9.1
VF	946	197.2	18.1

Table 2. Patterns of component ratio of each rhythm

	Pattern 1	Pattern 2	Pattern 3	Pattern 4
SR	random	25%	40%	55%
SVT	random	25%	20%	15%
VT	random	25%	20%	15%
VF	random	25%	20%	15%

〈2・2〉 不整脈の分類方法 本研究では，4種類の心調律の状態（SR，SVT，VT，VF）の判別を行うために，次のような，心内心電図の特徴量より得られる複数の指標を入力とした重回帰モデルに基づく方法を用いた[9][10]。

いま，上述のデータ窓における0.2 sの各シフトによって増加する離散時間をkとする。各データに対して，後述するm個の指標を求め，これらを要素とする$m \times 1$ベクトルを$\boldsymbol{x}(k)$とおく。また，4種類の心調律の種類SR，SVT，VT，およびVFに対応する番号をそれぞれ$i = 1, \ldots, 4$とするとき，心調律の分類を

$$y_i(k) = \begin{cases} 1 & \text{(if the sample belongs} \\ & \text{to the rhythm } i\text{)} \\ 0 & \text{(otherwise)} \end{cases} \quad \cdots\cdots (1)$$

で表す。$y_i(k)$を要素とする4×1ベクトル$\boldsymbol{y}(k) = [y_1(k), \ldots, y_4(k)]^{\mathrm{T}}$を検出ベクトルと呼ぶこととする。データベクトル$\boldsymbol{x}(k)$を説明変数とし，検出ベクトル$\boldsymbol{y}(k)$を目的変数とする重回帰モデルを

$$\boldsymbol{y}(k) = \boldsymbol{A}\boldsymbol{x}(k) + \boldsymbol{e}(k) \cdots\cdots (2)$$

で表す。ここで，$\boldsymbol{A}$は$4 \times m$行列であり，4×1ベクトル$\boldsymbol{e}(k)$は残差である。

本研究では，先行研究において実験的に有効性が確認された条件として，指標の数を$m = 14$，データ窓の個数を$K = 400$と定め，最小二乗法により(2)式の重回帰モデルの係数行列$\boldsymbol{A}$を計算した。

運用時には，逐次的に計算した各指標から作られる$\boldsymbol{x}(k)$を，(2)式で$\boldsymbol{e}(k) = 0$としたモデルに入力し，SR，SVT，VT，およびVFに対応する4つの目的変数$\boldsymbol{y}(k)$の推定値として検出結果ベクトル$\hat{\boldsymbol{y}}(k)$を計算する。それらの中の最大値に対応する心調律の番号iを，その時の心調律の種類として判定する。

先行研究では，全部でW個のデータ窓から無作為にK個のトレーニングデータを選択していたため，データ数の少ない心調律がトレーニングデータとして選ばれる確率は低かった。特にSVTは他の心調律に比べてデータ数が少なく，先行研究ではSVTの感度が低いモデルが推定されていた。そこで，本研究では，各心調律のトレーニングデータの割合をTable 2のような4種類のパターンを設定し，重回帰モデルの推定を行った。なお，Pattern 1は，先行研究で用いられている方法である。W個のデータをテストデータとし，推定された重回帰モデルの妥当性を検証するために用いた。

〈2・3〉 心内心電図に基づく指標 本研究では，重回帰モデルの入力として，先行研究[9][10]と同様，以下に示す14個の特徴量を用いた。

（1） Histogram: 心房と心室における心電図信号間の2次元ヒストグラムから求められる，Pearsonのχ^2統計量および標準偏差σ

（2） Period: $IECG_{\mathrm{LV}}$，$IECG_{\mathrm{RV}}$および$IECG_{\mathrm{RA}}$から得られる心周期とそれぞれの心周期間の比

（3） Delay: 2つの心電図間のR波検出における相対的な遅れ時間

（4） Complex: 2つの心電図をそれぞれ実部と虚部とする複素数と見なしたときの偏角と絶対値から求められる指標

〈2・4〉 過去の時系列を考慮した不整脈検出 本研究では，ある判定対象であるk番目の窓に対して，$\hat{\boldsymbol{y}}(k)$の最大値$\hat{y}_{\max}$が，あるしきい値$\hat{y}_{th}$より小さい場合，(3)式のように，その窓から過去n個の窓における検出結果ベクトルの値$\hat{\boldsymbol{y}}(k)$の平均を算出して判定を行う自己回帰フィルタを用いた。

$$\hat{\boldsymbol{y}}(k) \leftarrow \frac{\hat{\boldsymbol{y}}(k) + \hat{\boldsymbol{y}}(k-1) + \cdots \hat{\boldsymbol{y}}(k-n+1)}{n} \cdots\cdots (3)$$

この方法により，$\hat{y}_{\max}$が小さく信頼性が低い分類結果に対して，過去の判定結果の影響を及ぼすことで，誤判定を減らすことができると推察される。

本研究では，各パターンにおいて，致死性不整脈の不検出が最小，すなわち後述の偽陰性率が最小となるようなnを選択した。また，しきい値$\hat{y}_{th}$は，VFの不検出が起こる範囲に基づき，$\hat{y}_{th} = 0.7$と設定した。

加えて，VFの不検出を減らすために，複数窓の判定結果から1つの判定結果を確定する方法を導入する。先行研究[9][10]では窓のシフト幅である0.2 sごとに判定結果を出力していたが，本研究ではt_{det} [s]ごとに判定結果を出力する方法を検討する。提案方法では，複数個の窓における判定結果に対し，多数決関数を用いることで，1つの判定結果を$t_{\mathrm{det}} = 0.2, 0.4, \ldots, 3.0$ [s]ごとに出力することとした。この方法により，例えばVFの判定の中に突発的に出現したSRなどの誤判定を取り除くことができると考えられる。

〈2・5〉 検出性能の評価方法 提案アルゴリズムの有効性を評価するために，$W = 5213$個のデータ窓から，Table 2の4種類のパターンに基づいて，$K = 400$個の

窓で区切られたトレーニングデータを選択し，重回帰モデルを推定した。さらに，提案方法のロバスト性を評価するため，先行研究[9][10]と同様にこの操作を100回繰り返し行い，偏回帰係数の平均値を算出することで平均モデルを求めた。そして，平均モデルを用いて全データ（$W = 5213$個）を対象とした心調律の分類を行った後，自己回帰フィルタを用いた分類および複数個の窓に対し多数決関数を用いた分類を段階的に適用した。

本研究では，自己回帰フィルタ適用後の判定結果と複数個の窓に対し多数決関数を用いたときの判定結果を個々に算出し，それぞれの提案方法に対する有効性の検証を行った。

それぞれのアルゴリズムの分類性能の評価を行うため，分類結果におけるそれぞれの心調律の感度と特異度を算出した。また，ICDが作動する場合（VT，VF）とそうでない場合（SR，SVT）に分けることで，偽陽性率および偽陰性率を算出し評価を行った。ここで，偽陽性率は誤分類によってICDが誤作動を起こす確率であり，SRとSVTのうちVTもしくはVFと誤って判定した窓数をSRとSVTの総窓数で割ることで算出される。一方，偽陰性率は誤分類によって致死性不整脈を見落とす確率であり，VTとVFのうちSRもしくはSVTと誤って判定した窓数をVTとVFの総窓数で割ることで算出される。

3. 結　果

まず，重回帰モデル推定後に自己回帰フィルタを適用して得られた分類結果のうち，各パターンにおける特異度をFig.3，感度をFig.4，偽陽性率ならびに偽陰性率をFig.5に示す。

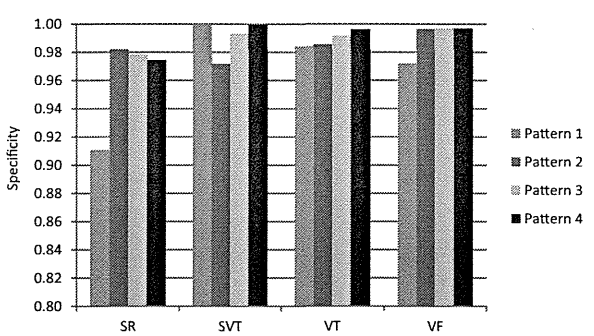

Fig. 3. Specificity of classification calculated from 4 pattern models

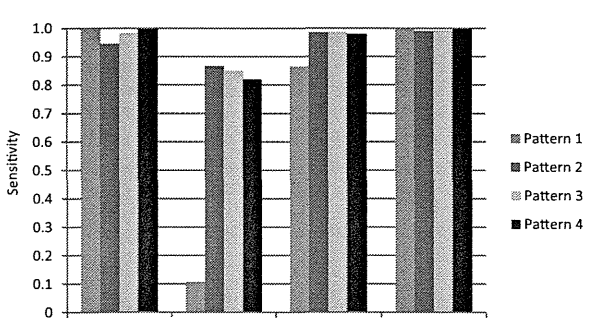

Fig. 4. Sensitivity of classification calculated from 4 pattern models

次に，自己回帰フィルタを適用した後に多数決関数を用いた複数個の窓の判定を行った場合の分類結果について，t_{det}を変化させたときの偽陽性率の変化をFig.6，偽陰性率の変化をFig.7に示す。

4. 考　察

Fig.3より，Pattern 1に比べてPattern 2〜4の方がSR，VT，VFの特異度が高いことがわかる。一方，SVTについてはPattern 2〜4の方が低い値であるが，これは，Pattern 1のときは，SVTが正しくモデル化できておらず，SVTと

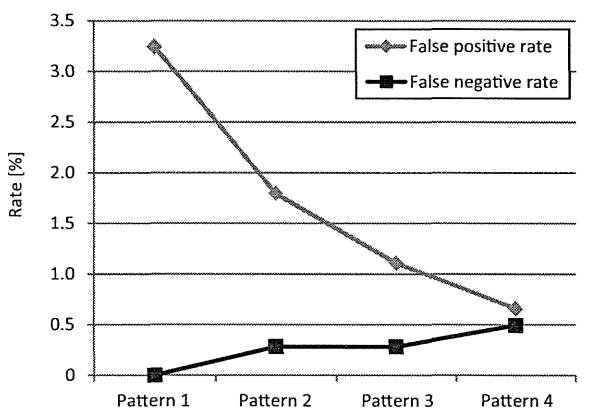

Fig. 5. False positive rate and false negative rate of classification calculated from 4 pattern models

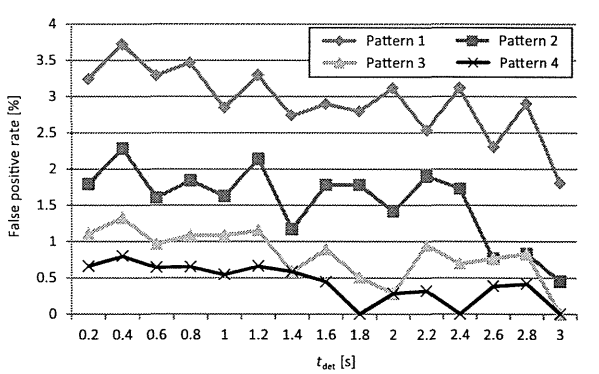

Fig. 6. False positive rate of classification using multiple windows

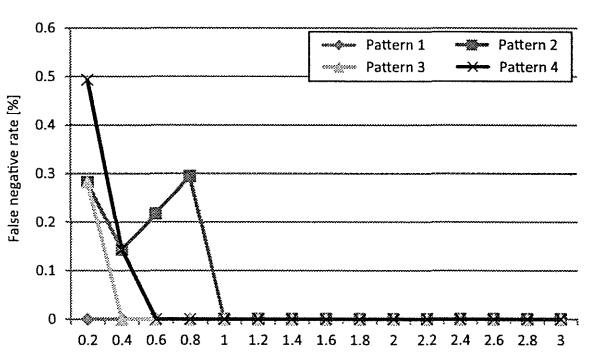

Fig. 7. False negative rate of classification calculated from 4 pattern models

判定される窓の数が少ないためである。

同様に，Fig.4 より，SR の比率を大きくすることで，SVT，VT の感度が上昇することがわかる。特に，SVT の感度の大幅な上昇がみられ，SR の比率を変更するというモデルの作成方法における有効性が確認された。

上述の結果から推察できるように，偽陽性率に関しては，Fig.5 より，Pattern 1 に比べて Pattern 2〜4 では低下する結果となり，SR や SVT の誤判定が減少している。一方で，偽陰性率に関しては，SR の比率の上昇とともに高くなる傾向があり，VF の不検出といった重大な誤判定が増加する可能性がある。

以上から，従来法に加えて，自己回帰フィルタを用いた解析方法では，Pattern 2〜4 において，SR や SVT の誤判定による ICD の誤作動が大幅に少なくなるものの，VF の不検出を伴う可能性があり，ICD への実装を考慮すると不十分な判定法であると考えられる。

次に，その問題点を解決する方法として用いた，多数決関数による複数個の窓の判定結果に基づく分類方法の結果について考察する。

Fig.6 より，t_{det} が大きくなるにつれて，偽陽性率は低下する傾向となった。また，SR の比率が大きいほど偽陽性率は低くなり，特に Pattern 4 では，$t_{\mathrm{det}} = 1.8$ [s] のとき 0 となる。一方，Pattern 1〜3 では偽陽性率が 0 となるには 3 s 以上必要となるか，または 0 にならないため，Pattern 4 によるモデル作成方法の優位性が確認できる。

一方，偽陰性率については，Fig.7 より，$t_{\mathrm{det}} = 1.0$ [s] のときすべての Pattern で 0 となり，提案手法によって VF 不検出の問題点が解消されていると考えられる。

これらの結果より，多数決関数を用いた複数個の窓による分類方法は，分類が確定するまで 1 s 程度の時間を要するものの，偽陰性率を 0 にし，偽陽性率を減少させることができる有用な方法であることが示された。特に Pattern 4 では $t_{\mathrm{det}} = 1.8$ [s]，すなわち 9 個の窓の判定結果による多数決のときに偽陽性率，偽陰性率ともに 0 となり，有効性の高い手法であると推察される。さらに，既存の ICD の検出時間が 2〜3 s 程度[11][12]であることと比較して，致死性不整脈を早期に検出することが可能であるといえる。

これらの結果は，モデル作成に用いられるトレーニングデータにおける，心調律の比率による影響も大きいと考えられる。従来法で用いられた Pattern 1 のような無作為にテストデータを抽出する方法では，全データに含まれる心調律の比によってテストデータにおける心調律の比が決まる。そのため，全データに含まれる SVT や VT のような心調律の割合が小さい場合には，それらの心調律の特徴を十分に表すモデルを作成することが難しい。一方，本研究の提案方法では，4 つの心調律を特定の割合でテストデータとすることで，それぞれの心調律を特徴づける有効性の高いモデルを作成できたと推察される。

ただし，提案方法には次のような問題点もある。本方法では，重回帰モデルによる出力が正しい判定結果を示している場合においても，多数決関数の処理を行ってしまうため，冗長性が生じる可能性がある。そのため，VF 不検出に対する性能と処理の冗長性の関係について今後検討する必要がある。

5. おわりに

本研究では，不整脈の割合が SR に比べて小さいデータ群において，誤検出の少ない重回帰モデルの作成方法を提案した。また，VF の不検出や ICD の誤作動となる誤分類を減らすために過去の時系列を考慮した方法を提案した。提案した重回帰モデルの作成方法では，特に SVT や VT のようなデータ数の少ない心調律の検出精度の向上が認められた。さらに，自己回帰フィルタと多数決関数を適用することで，VF の不検出率を 0 に近づけることができ，偽陽性率を低下させることが可能となった。

提案したアルゴリズムについて，大幅な検出性能の向上が認められるが，論理的な複雑性から計算量の増加が問題となる可能性がある。そのため，ICD への実装を行う際には，計算量を抑える工夫を行って有効性を検証する必要がある。その検証の際には，重回帰モデルにおいて説明変数である指標の個数はどのくらいが最適であるか検証する必要がある。加えて，本研究で取り扱った 4 種類の心調律以外のデータに対しても，アルゴリズムがどのように動作するか検証をする必要性があると考えられる。

文　献

（1） 笠貫　宏：植込み型除細動器 (ICD) の歴史。日本心臓ペーシング・電気生理学会，植込み型除細動器調査委員会編，植込み型除細動器の臨床。医学書院，東京，p.1 (1998)

（2） 杉本恒明：突然死と不整脈。杉本恒明編，不整脈学。南江堂，東京，pp.12–14 (1992)

（3） A. Bayes de Luna, P. Coumel, and J.F. Leclercq: “Ambulatory sudden cardiac death: mechanisms of production of fatal arrhythmia on the basis of data from 157 cases”, *Am. Heart J.*, Vol.117, No.1, pp.151–159 (1989)

（4） M. Mirowski, M.M. Mower, and P.R. Reid: “The automatic implantable defibrillator”, *Am. Heart J.*, Vol.100, No.6, pt.2, pp.1089–1092 (1980)

（5） 大西　哲・笠貫　宏：ICD の原理と構造。田中茂夫編，心臓ペースメーカー・植込み型除細動器。メジカルビュー社，東京，pp.154–171 (2001)

（6） E. Aliot, R. Nitzsche, and A. Ripart: “Arrhythmia detection by dual-chamber implantable cardioverter defibrillators. A review of current algorithms”, *Europace*, Vol.6, pp.273–286 (2004)

（7） K. Nanthakumar, M. Paquette, D. Newman, D.C. Deno, L. Malden, B. Gunderson, J. Gilkerson, M. Greene, D. Heng, and P. Dorian: “Inappropriate therapy from atrial fibrillation and sinus tachycardia in automated implantable cardioverter defibrillators”, *Am. Heart J.*, Vol.139, pp.797–803 (2000)

（8） C. W. Israel: “How to avoid inappropriate therapy”, *Current Opinion in Cardiology*, Vol.23, No.1, pp.65–71 (2008)

（9） 阿部　誠・テルマ　ケイコ　スガイ・吉澤　誠・山家智之・清水一夫・後藤　萌・稲垣正司・杉町　勝・砂川賢二：「重回帰分析を用いた致死性不整脈検出アルゴリズムに関する検討」，生体医工学，Vol.48, No.6, pp.577–583 (2010)

（10） 阿部　誠・テルマ　ケイコ　スガイ・吉澤　誠・本間経康・杉田典大・清水一夫・後藤　萌・稲垣正司・杉町　勝・砂川　賢二：植込み型除細動器用致死性不整脈検出アルゴリズムの高速・高精度化，生体医工学，Vol.49, No.6, pp.932–938 (2011)

(11) M. Nair, N. Saoudi, D. Kroiss, and B. Letac: "Automatic arrhythmia identification using analysis of the atrioventricular association", *Circulation*, Vol.18, No.95, pp.967–973 (1997)
(12) E. G. Daoud, K. Nademanee, C. Fuenzalida, G.F. Tomassoni, C. Schuger, M. Chisner, M. Simones, M. Schwartz, and H. Reeve. "Clinical experience with tiered atrial therapies and atrial arrhythmia prevention algorithms in a dual chamber cardioverter defibrillator", *Journal of Cardiovascular Electrophysiology*, Vol.17, pp.852–856 (2006)

阿　部　　誠　（正員）　2009 年東北大学大学院工学研究科博士後期課程修了。同年同大学サイバーサイエンスセンター厚生科研費研究員，11 年同大学工学研究科助教，現在に至る。映像の生体影響評価，致死性不整脈検出アルゴリズムの開発に関する研究に従事。博士（工学）。

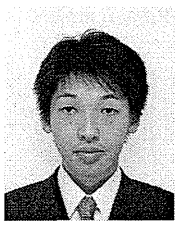

吉　澤　　誠　（非会員）　1983 年東北大学大学院工学研究科博士後期課程修了。同大学工学部助手，助教授，豊橋技術科学大学助教授，東北大学大学院助教授，同大学情報シナジーセンター教授を経て，現在，同大学サイバーサイエンスセンター教授。モバイル健診装置の開発に関する研究等に従事。工学博士。

テルマ　ケイコ　スガイ　（非会員）　2011 年東北大学大学院医工学研究科博士後期課程修了。致死性不整脈検出アルゴリズムの開発，補助人工心臓装着時における心機能推定に関する研究に従事。博士（医工学）。

本　間　経　康　（非会員）　1995 年東北大学大学院工学研究科博士後期課程修了。2000 年 Saskatchewan 大学客員教授などを経て，2003 年東北大学医学部助教授，2008 年同大学サイバーサイエンスセンター准教授，現在に至る。最適制御，複雑系，脳科学，医用画像等の研究に従事。博士（工学）。

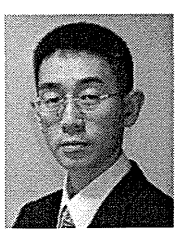

杉　田　典　大　（非会員）　2004 年東北大学大学院工学研究科博士後期課程修了。2005 年，21 世紀 COE フェロー，2006 年，同大学工学研究科助手，助教を経て，現在，同大学工学研究科准教授。映像等の生体影響評価に関する研究等に従事。博士（工学）。

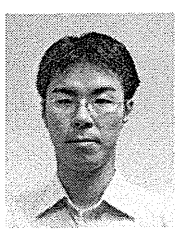

清　水　一　夫　（非会員）　1983 年長岡技術科学大学大学院電気電子システム専攻科修了。1988 年オリンパス (株) 中途入社第 2 開発部所属，1998 年同社新事業推進本部 DM-pj グループリーダー（課長），同社研究開発企画部課長を経て，現在，同社医療技術開発本部医療探索部部長。医療機器の研究開発に従事。

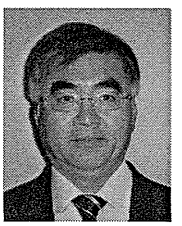

後　藤　　萌　（非会員）　2009 年東京大学大学院工学研究科修士課程修了。同年，オリンパス (株) 入社。現在，オリンパス株式会社医療技術開発本部医療探索部研究員。専門分野は生体信号処理。

稲　垣　正　司　（非会員）　1987 年千葉大学医学部卒業。同年同大学医学部付属病院勤務，1991 年国立循環器病センター内科心臓部門，1996 年同研究所循環動態機能部研究員を経て，現在，国立循環器病研究センター研究所循環動態制御部室長。専門分野は循環器病学，不整脈学。

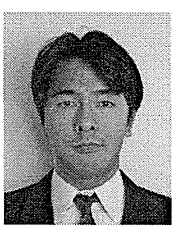

杉　町　　勝　（非会員）　1984 年九州大学医学部卒業，1992 年論文博士取得。同年，国立循環器病センター研究所室長，2004 年同研究所部長を経て，現在，国立循環器病研究センター研究所循環動態制御部部長。心臓力学，循環動態，循環制御の研究，医療機器開発等に従事。博士（医学）。

砂　川　賢　二　（非会員）　1974 年九州大学医学部卒業。論文博士取得。同大学医学部循環器内科医員，ジョンズホプキンス大学医学部研究生，講師，助教授，九州大学医学部助手，講師，国立循環器病センター研究所循環動態機能部長を経て，現在，九州大学大学院医学研究院循環器内科教授。専門分野はバイオニック心臓病学，心血管の力学等。医学博士。

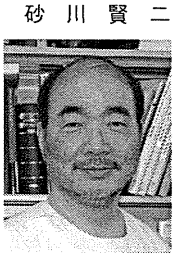

INVITED PAPER *Special Section on Medical Information Communication Technology for Disaster Recovery and Human Health Care Support*

Application of a Telemedical Tool in an Isolated Island and a Disaster Area of the Great East Japan Earthquake

Makoto YOSHIZAWA[†a)], **Tomoyuki YAMBE**[††], **Norihiro SUGITA**[†††], **Satoshi KONNO**[††], **Makoto ABE**[†††], **Noriyasu HOMMA**[†], **Futoshi TAKEI**[††††], **Katsuhiko YOKOTA**[†††††], **Yoshifumi SAIJO**[††††††], ***and*** **Shin-ichi NITTA**[*], ***Nonmembers***

SUMMARY The present paper has reported a case study of the "Electronic Doctor's Bag" which is a telemedical tool for home-visit medical services using the mobile communications environment in an isolated island and a disaster area hit by the tsunami. Clinical trials performed for 20 patients around a clinic in Miyako Island indicated that the communication functions of the proposed system were highly evaluated by patients as well as medical staffs. However, the system still has room for further improvement in operability, portability and mobile communication environment. The experience at the shelter in Kesennuma City suggested that mobile healthcare tools such as the proposed system will be strongly required when there are no or only paramedical staffs after leaving of emergency medical staffs.

key words: *the Great East Japan Earthquake, telemedicine, isolated island, disaster area, mobile communication*

1. Introduction

On March 11, the giant tsunami in the Great East Japan Earthquake hit the coastal areas of Tohoku district and fully destroyed their environment of life. For several months after the tsunami, the disaster victims who lost their houses were forced to live in shelters such as school gymnasiums with a horrible environment. Currently almost all the victims have moved to temporary houses whose healthcare environment is not always good.

However, the healthcare environment in Tohoku region has already been in a critical state because the uneven distribution of medical doctors has been widened due to an aging and declining population. It can be easily predicted that the disaster will accelerate the deterioration of this serious problem.

On the contrary, this case will become a touchstone for solution of the same problem as all other rural areas in Japan as well as Tohoku region are facing. The use of information and communication technology (ICT) may be a possible solution for such issues.

To prevent crisis in the nation's deficit-ridden health insurance system, the Japanese government is promoting the policy of home medical care. The healthcare insurance reform in 2006 newly established the home care support clinic system which intends to spread the clinics operating house visit services on 24-hour schedules [1].

However, in the case of a small clinic, a doctor may be forced to work in sleepless and hard working environment and the doctor's transportation time to patients' homes reduces the efficiency of medical care. Moreover, the remuneration for medical services decided by the system is not enough to spread the home care support clinics.

In this situation, Tohoku University established a consortium "The Consortium for Medical Information Communications System in the Mobile Environment" on March 4, 2009. The main purpose of this consortium is to provide the ubiquitous communications system not only for home-visit medical services but also for mass health examination, emergency care, and disaster areas. In collaboration with the Sendai Area Knowledge Cluster Initiative supported by the Ministry of Education, Science, Culture and Sports in Japan, the consortium developed a prototype of communications system, named "Electronic Doctor's Bag" in 2009. After evaluation of its function at a few clinics [2], a new version has newly developed in 2010 as shown in Fig. 1.

The purpose of this system is that instead of a doctor, a nurse carries the Electronic Doctor's Bag and visits

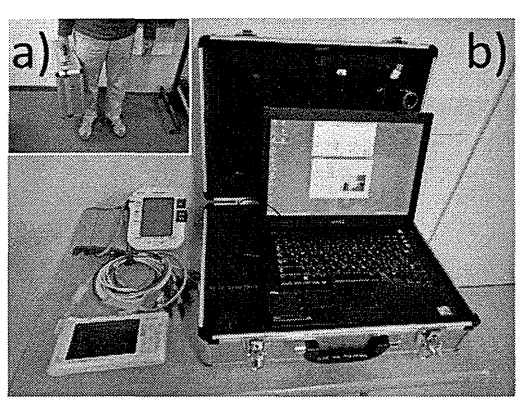

Fig. 1 Electronic Doctor's Bag. a) Carrying mode. b) Operation mode.

Manuscript received January 31, 2012.
Manuscript revised March 21, 2012.

[†]The authors are with Cyberscience Center, Tohoku University, Sendai-shi, 980-8578 Japan.
[††]The authors are with Institute of Development, Aging and Cancer, Tohoku University, Sendai-shi, 980-8574 Japan.
[†††]The authors are with the Graduate School of Engineering, Tohoku University, Sendai-shi, 980-8579 Japan.
[††††]The author is with Umyaasu N Clinic, Miyakojima-shi, 906-0013 Japan.
[†††††]The author is with Tokyo Denki University, Tokyo, 101-8457 Japan.
[††††††]The author is with the Graduate School of Biomedical Engineering, Tohoku University, Sendai-shi, 980-8579 Japan.
[*]The author is an emeritus professor of Tohoku University.
a) E-mail: yoshizawa@isc.tohoku.ac.jp
DOI: 10.1587/transcom.E95.B.3067

a patient's home but an equivalent face-to-face communication between the doctor in his or her clinic and the patient at home can be realized by sending biological information with multiple high-definition images.

This paper will report the results of field tests of the proposed telemedical tool applied in an isolated island and a disaster area of the Great East Japan Earthquake.

2. Methods

2.1 Basic Function of Electronic Doctor's Bag

Figure 2 shows the framework of the Electronic Doctor's Bag. First, personal verification of the patient is done with a vein authentication to avoid mixing-up among patients. Secondly, to verify the patient's state such as complexion, movement and gait, his high resolution video picture is taken, highly compressed and coded for preserving individual security in a real time fashion. This signal is sent to the medical doctor staying in his own clinical office via a mobile communications system of cellular phones and the Internet.

The main targets of the proposed system are general chronic diseases such as circulatory disease, diabetes and the respiratory organ disease. Not only patient's high-definition video image to doctors to provide just like face-to-face examination but also various kinds of biological data are measured with an electrocardiographic (ECG) monitor, a blood-pressure meter, a blood sugar level meter and an ultrasonic diagnostic system. These data are connected directly with the main body of the Bag via USB interface or wireless communication line and also compressed, coded and sent to the doctor as automatically as the nurse does not need any cumbersome procedure. The ubiquitous system can be used in places without the Internet access, including ordinary households or moving vehicles such as ambulance cars.

2.2 New Features of Electronic Doctor's Bag

The system has following new features in comparison with the previous version [3].

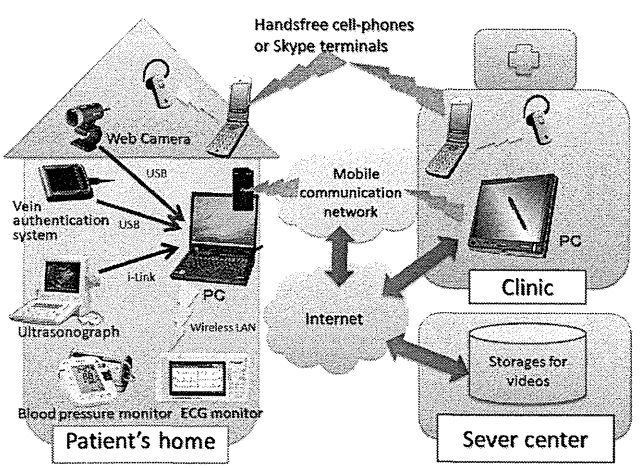

Fig. 2 Framework of the Electronic Doctor's Bag.

1) The PC for transmission
A high performance laptop computer was used. For mobile Internet access, E-mobile 3G (D31HD; Upstream: 5.8 Mbps, Downstream: 21 Mbps) and Willcom CORE 3G (HX006ZT; Upstream: 5.7 Mbps, Downstream: 7.2 Mbps) were used However, it is assumed that any clinic can have sufficiently high Internet access such as an ADSL or a fiber-optic network. The whole system measures 475 × 355 × 185 mm and weighs 8 kg.
2) 12-lead electrocardiographic monitor (Fukuda Denshi; ESP-300DX/SP)
A wireless LAN was used for sending data to the PC after monitoring to enhance operability.
3) Ultrasonographic monitor
A High resolution-type portable ultrasonographic unit (Honda Electronics; HS-2100) was used and its video output signal was acquired with the video capture box to be sent to the PC. Moreover, an ultra-compact ultrasonographic unit (GE; Vscan) was used in an off line fashion.
4) Web camera
A digital video camera (1080 p) used in the previous version had high performance such as a function to avoid blurring of images due to hand movement. However, the camera was heavy and not easy to handle. A Web camera (Microsoft; LifeCam Cinema; 720 p) with lower weight and cost has been adopted to improve operability.
5) Conversation tool
Not only at the clinic but also at patients' homes, video terminals for Skype (ASUS; AiGuru SV1T) were used to hold a conversation among the patient, his or her family, the nurse and the doctor with a low-definition video image (monochrome, 640 × 480 pixels) as well as a high-definition image (color, 1080 p) provided by the Bag.
6) Personal authentication
A vein authentication tool (Sony; FVA-U1) was used to identify patients, nurses and doctors. Such a biometric tool is useful for avoiding mixing-up among patients and preventing unauthorized persons from accessing patients' individual information.
g) Data server
A data server is placed in Tokyo and working to preserve the data sent from the PC in patients' homes. This has enabled the plural doctors to refer and share the patients' present data as well as the past one. The size of the server is 430 GB and ensures records of over 3,000 hours with the present resolution of the video signal captured by the system. It is easy to extend the size of the server.
7) Data access of the PC as a receiver
In the previous version, a gateway named "Digital Gate" made by Sony Co. was needed to receive the

encrypted data. In the current version, any PC that can access the Internet has been able to receive the data if the PC is installed with the certification software to certify the right of access to the information. This process has enabled the plural doctors to receive the data of the same patient simultaneously in anywhere all over the world by accessing the server in the Internet without loss of security. This function will be able to promote establishment of a cooperation network among doctors.

8) Display function of the PC as a receiver
Both of the video image of the ultrasonographic monitor and the video image of the Web camera can be displayed simultaneously on the PC for receiving the data. This function has enabled the doctor to watch the echo image, ascertaining the position and the posture of the probe operated by the nurse.

2.3 Application in an Isolated Island

In general, the healthcare environment of isolated islands is not good due to geographical conditions. In an isolated island, it is likely that residents have a bad access to hospitals and that a doctor and an insufficient number of healthcare professionals are forced to perform a heavy medical practice, coping with a sense of isolation under less up-to-date medical information.

The Electronic Doctor's Bag is suitable for improvement of the healthcare environment of isolated islands. This system will be able to save the cost and time for transportation if the nurse visits patients' home with the Bag instead of the doctor.

To ascertain the above thought, the experiment was performed at total 20 patients' homes around "Umyaasu N Clinic" (Director: Dr. Futoshi Takei) in Miyako island, Okinawa Prefecture for 20 days from October 20th, 2010 to November 10, 2010.

The following items were preliminarily evaluated for a nurse with a simulated patient before carrying out the main experiments using actual patients.

1) To check the mobile communication environment of the patients' home.
2) To understand how to carry and deal with the equipment.
3) To learn the procedure of preparation, operation, data transmission and communication with the doctor.
4) To understand the purpose of the operational protocols related to ordinary healthcare treatments.
5) To learn how to get an informed consent from the patients and their family.
6) To learn remote indication and instruction from the doctor.
7) To check the adequacy of conversation among the patient, the nurse and the doctor through remote communication devices.
8) To check the adequacy of healthcare treatments according to kinds of diseases under remote instruction from the doctor.
9) To learn how to record the procedure of the experiment.

After the preliminary evaluation, patients satisfying the following conditions were used to apply the proposed system.

- The patients who have been receiving the home visit medical services or who do not easily go to the clinic.
- The patients who have indication for ECG, blood pressure or ultrasonographic examination.
- The patients who can be diagnosed with the transmitted video or still images.
- The patients who have chronic diseases such as cardiovascular diseases, diabetics or cerebral stroke, etc.

In the experiment with actual patients, the following items were evaluated.

10) For the doctor

a) To check if the doctor can clearly read ECG, blood pressure and ultrasonographic data, comparing with the original data measured at the patient's home.
b) To check the followings on the basis of the transmitted video image.
   - The state of attaching the electrodes of the ECG monitor.
   - The state of attaching the cuff of the blood pressure monitor.
   - The position and attitude of the probe of the ultrasonographic monitor.
   - The effect of motion of the camera operated by the nurse on visibility of the video image.
c) To check the followings on the basis of the transmitted sounds.
   - Quality and delay of sounds.
   - Ability of conversation among attendants.
   - Ability of instruction from the doctor to the nurse.

11) For the nurse and the patient
In addition to the above items for the doctor, the followings were evaluated.
   - To check if the camera can be set at an appropriate position to take the state of the patient as soon as possible.
   - To check if the camera can be successfully moved according to the instruction from the doctor.
   - To check if the nurse can operate the PC of the Bag even at the patient's home.
   - To check if the patient and his or her family feel uneasy due to unfamiliar equipment and strange operation.

The above all items were evaluated with questionnaires asked to the doctor, the nurse and patients.

2.4 Application in a Disaster Area

Moreover, the proposed system was also applied in a disaster area hit by the tsunami of the Great East Japan Earthquake. On June 18, 2011 at the shelter of the gymnasium of Hashikami Junior High School in Kesennuma City, Miyagi prefecture, Japan, the Bag was used for health consultation of 17 people of the victims. The place was a temporary healthcare room that had been a preparation room for sporting equipment. The doctor, Dr. Tomoyuki Yambe, was at the laboratory of the Department of Medical Engineering and Cardiology, Institute of development, Aging and Cancer, Tohoku University, Sendai City, Japan.

3. Results

3.1 Application in an Isolated Island

Mobile communication quality

Around "Umyaasu N Clinic", Willcom Core 3G was not stable and about 60 kbp upstream at most. On the other hand, E-mobile 3G was sufficient for communication because it attained about 250 kbps upstream and 3.8 Mbps downstream. The most severe problem was that almost all patients' houses were built of concrete against typhoons, and thus it was difficult for radio waves to penetrate through the wall into the room where the Bag worked.

Evaluation of the adequacy of the proposed system

Figure 3 shows a scene of measuring blood pressure at the clinic using a simulated patient. It was ascertained that the almost all preliminary items 1)–9) shown in 2.3 were successfully evaluated by the nurse.

In the actual clinical trials, the nurse visited total 20 patients with cerebral infarction, cerebral hemorrhage, chronic endocranium, Alzheimer's dementia, aphasia, Parkinson's disease, depression, cardiac noise, expansion type cardiomyopathy, hypertension, hyperlipidemia, hypercholesterol, metabolic syndrome, diabetes, glucose tolerance obstacle, SAS, bloody bowel discharge tumor, hyperuricemia, bone fracture, arthropathy, gonarthrosis, congenital scoliosis, back pain, uneasy walk, pigmentary degeneration of the retina, etc. Most of them were accompanied by complications. It was also confirmed that the almost all items 10) and 11) for the experiment using the actual patients were successfully evaluated except some parts shown below.

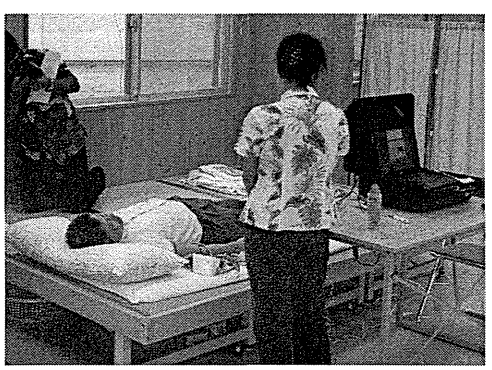

Fig. 3 Measurement of blood pressure with the Electronic Doctor's Bag at "Umyaasu N Clinic" using a simulated patient.

The function of almost automatic transmission of biological data, i.e., ECG and blood pressure, was highly evaluated by the nurses. However, they assessed that the procedure of setting of the video camera and connection among the main body, the peripheral devices and the electrical power units should be improved to be done in a much simpler way. In particular, it could be found that setting and operation of the video camera may prevent the nurse from taking care of the patient and performing other usual medical tasks.

It could be verified that the transmitted high-definition video image from the Bag was very useful for the patient's state from the view point of the doctors. On the other hand, the doctor and the nurse indicated that the Skype terminals were also useful for conversation in a similar face-to-face fashion due to bidirectional communication but not suitable for diagnosis and precise instruction from the doctor to the nurse.

Moreover, the patients and their family told comments, which were described in questionnaires, as follows:

- I really impressed by the fact that I can face and talk with the doctor using the TV phone.
- I think this system will be very good unless the Skype works intermittently.
- I am happy to take the health check while sitting in my own home.

3.2 Application in a Disaster Area

Figure 4 shows the photos taken at the temporary healthcare room of the shelter of the gymnasium of Hashikami Junior High School in Kesennuma. At that time, about three months had passed from the Earthquake but the shelter was full of victims as shown in Fig. 4(a). Figure 4(b) represents a scene of the tele-consultation of a patient with the doctor in Sendai about 100 km far from Kesennuma. As shown in Fig. 4(c), another patient holds a conversation with the doctor through the Skype terminals. In this case, the communication line was not the mobile communication but the temporary Internet cable provided by a communication company without any charge. Figure 4(d) shows a scene of the ultrasonographic diagnosis using the Vscan.

This ultrasonographic machine is so compact that the measurement was very easy even if the patient was lying on a mat spread out on the straw bed, which is a Japanese traditional type of room floor. Their surfaces were almost the same level. Unfortunately, the Vscan does not have an electrical outlet port of the video signal, and then the nurse was forced to take the display screen of the Vscan with the camera of the Bag to send to the doctor. Of course, the res-

Fig. 4 Application of the proposed system at the shelter using a gymnasium in Kesennuma. a) Whole view of the shelter, b) Remote consultation assisted by a nurse, c) Conversation between a patient and a doctor far from there with Skype terminals, d) Use of an ultra-compact ultrasonographic unit.

olution of transmitted video image was reduced due to indirect shooting and the stability of the video frame was poor because the nurse took the video with the camera supported by only her hand without any tripod stand.

On the other hand, it could be verified that the high resolution color video transmission to the doctor was valid for consultation with a male patient complaining about pain at his hand because the doctor could judge his condition correctly.

4. Discussion

4.1 Application in an Isolated Island

It was not until we went to Miyako Island and actually performed the experiment that we found average private houses so bad in mobile communication environment. Miyako Island is an isolated island but a popular sightseeing place, and then we had considered that its mobile communication environment was better rather than rural and remote areas in the mainland. However, the ability of radio wave reception will be improved if a radio repeater is set around a window. On the other hand, in the case of extremely rural and remote areas such as mountain villages where mobile phones are out of service, the proposed system is, of course, invalid. The similar problem will happen if the proposed system is used in an ambulance car that may go to a poor reception area of radio wave.

In the literature [3], the authors pointed out the superiority of the proposed system to the other types of telehealthcare systems [4]–[9]. That is to say, the proposed portable high-definition video transmission system based on mobile communication is unique in comparison with other similar systems [7]–[9].

The results obtained from the clinical trials performed in Miyako Island indicates that only a low-definition TV meeting system or a TV phone like Skype terminals is not sufficient for precise medical diagnosis while the proposed system is useful due to both functions of high-resolution video image transmission and bidirectional audio and visual communication with cheap cost. However, it should be noted that the communication based on Skype has often been criticized for its weak security because of usage of P2P technology [10].

As shown in the patients' and their family's comments described in the questionnaire, they did not feel uneasy. This may be because the nurse was always with the patient and his or her family and she explained the procedure of the remote diagnosis. This fact suggests that home visit-type telemedical services will be easily accepted to at least patients.

4.2 Application in a Disaster Area

The results mentioned here were obtained from a temporary and transient situation such as the shelter about three months after the disaster. However, the situation changed rapidly than one might imagine in spite of the same disaster area. In the first several weeks, the healthcare situation was most sever and many doctors and paramedical staffs were strongly needed as well as emergency materials such as drags, foods, fuels, electricity and communication tools.

In this meaning, the proposed system will become useful a few or several months later when emergency medical teams had already gone but the healthcare environment around shelters or temporary houses remains poor. As already described above, the shelter we visited had a sufficiently fast fixed Internet access line at that time, and thus the mobile communication cards were not necessary. However, it is not realistic that all temporary houses in the disaster areas have the fixed line because the communication fee must be paid by oneself. In this case, similar healthcare units should be equipped at a house built as a community center in the temporary houses, or some healthcare cars equipped with clinical instruments and mobile communication lines should visit there with paramedical staffs instead of a doctor.

Currently, smartphones and tablet PCs have spread drastically into many people. In addition, the speed of mobile communications lines is getting higher, for example, the next generation WiMAX (IEEE802.16 m) will be 350 Mbps in the best effort. This stream enables us to guess that in the future, patients as well as doctors will think of mobile healthcare as a matter of course. The key to the promotion of the mobile healthcare may be to develop various kinds of light, compact and portable medical devices linked wirelessly to smartphones or tablet PCs, and more simple, precise and cheap personal authentication units are required. It is also important to develop groupware to collaborate among doctors and paramedical staffs with a high security level after some related legal deregulation.

Judging from this tendency, the system developed here

can be regarded as a transitional prototype of a mobile healthcare tool in order to predict its idealized model in the near future.

5. Conclusions

The present paper has reported a case study of the "Electronic Doctor's Bag" which is a telemedical tool for home-visit medical services using the mobile communications environment in an isolated island, Miyako Island, and a disaster area, Kesennuma City hit by the tsunami.

Clinical trials of the proposed system were performed for total 20 patients around a clinic in Miyako Island. As a result, it was shown that both functions of high-resolution video image transmission and bidirectional audio and visual communication equipped in the proposed system were highly evaluated by patients as well as medical staffs. However, the system still has room for further improvement in operability and portability. In addition, we should cope with the poor radio wave environment inside private houses built of concrete.

At the shelter in Kesennuma, the proposed system was used for healthcare consultation for the victims with the doctor in Sendai. The experience suggested that mobile healthcare tools such as the proposed system will be strongly required when there are no or only paramedical staffs after leaving of emergency medical staffs.

Acknowledgments

The authors pray for an extraordinarily large number of victims of the Great East Japan Earthquake and Mr. Hiroshi Kawata who had dedicated himself to the progress of the present study but passed away immediately after the disaster. The authors thank staffs of Sony Business Solutions Co., Three Links Co., Fukuda Denshi Co., Honda Electronics Co., Willcom Co., Netone Co., Omron Healthcare Co. as members of The Consortium for Medical Information Communications System in the Mobile Environment, ICR Co., Sendai City and Miyagi Prefecture collaborating with the Sendai Area Knowledge Cluster Initiative.

References

[1] http://www.geocities.jp/onlinemedsante/zaitaku.html (in Japanese).
[2] M. Yoshizawa, T. Yambe, S. Konno, Y. Saijo, N. Sugita, T.K. Sugai, M. Abe, T. Sonobe, Y. Katahira, and S. Nitta, "A mobile communication system for home-visit medical services: The Electronic Doctor's Bag," Proc. 32nd Annu. Int. Conf. of IEEE EMBS, pp.5496–5499, Buenos Aires, Argentina, Sept. 2010.
[3] N. Sugita, M. Yoshizawa, T. Yambe, Y. Saijo, S. Konno, and S. Nitta, "Progress and evaluation of the Electronic Doctor's Bag," J. Jap. Telemed. and Telecare Assoc., vol.6, no.2, pp.207–210, 2010 (in Japanese).
[4] H. Hoenig, J.A. Sanford, T. Butterfield, P.C. Griffiths, P. Richardson, and K. Hargraves, "Development of a teletechnology protocol for in-home rehabilitation," J. Rehabil. Res. Dev., vol.43, no.2, pp.287–298, 2006.
[5] C.M. Cusack, E. Pan, J.M. Hook, A. Vincent, D.C. Kaelbe, and B. Middleton, "The value proposition in the widespread use of telehealth," J. Telemed. Telecare, vol.14, no.4, pp.167–168, 2008.
[6] M.A. Hebert, M.J. Paquin, L. Whitten, and P. Cai, "Analysis of the suitability of 'video-visits' for palliative home care: Implications for practice," J. Telemed. Telecare, vol.13, no.2, pp.74–78, 2007.
[7] J.C. Rosser, Jr, R.L. Prosst, E.B. Rodas, L.E. Rosser, M. Murayama, and H. Brem, "Evaluation of the effectiveness of portable low-bandwidth telemedical applications for postoperative followup: initial results," J. Am. Coll. Surg, vol.191, no.2, pp.196–203, 2000.
[8] K. Ogasawara, K. Ito, G. Jiang, A. Endoh, T. Sakurai, H. Sato, Y. Okuhara, T. Adachi, and K. Hori, "Preliminary clinical evaluation of a video transmission system for home visits," J. Telemed. Telecare, vol.9, no.5, pp.292–295, 2003.
[9] C. Yu, J.J. Yang, J.C. Chen, C.S. Liu, C.C. Chen, M.L. Lin, O.L. Liu, G. Yao, and C.W. Lin, "The development and evaluation of the Citizen Telehealth Care service System: Case study in Taipei," Proc. IEEE Eng. Med. Biol. Soc., pp.6095–6098, 2009.
[10] P. Wibmann, "Security review of the Skype network," Seminar at the Chair for Network and Data Security, Ruhr-University of Bochum, pp.1–13, Bochum, Germany, Jan. 2008.

Makoto Yoshizawa received the B.S., M.S. and Ph.D. degrees in Electrical and Communication Engineering from Tohoku University in 1978, 1980 and 1983, respectively. He was a Research Associate from 1983 to 1991 in the same department. Since 1991 to 1994, he was an Associate Professor in Toyohashi University of Technology, Toyohashi, Japan. In 1994, he returned to Tohoku University. He became a Visiting Scientist, Research Institute of Medicine, Johns Hopkins University, Baltimore and Baylor College of Medicine, Houston, U.S.A. in 1999. Since 2001, he has been a Professor in the Research Division on Advanced Information Technology, Information Synergy Center (currently, Cyberscience Center), Tohoku University. He engages in application of virtual reality to medicine, intelligent control of artificial hearts, assessment of effects of visual stimulation on humans and tele-healthcare. From 2005 to 2007, he was a Director of Finance of the Society of Instrument and Control Engineers. He was a member of AdCom of IEEE EMBS From 2009 to 2011. He has been a member of Editorial Committee and a councilor of Journal of the Japanese Society for Medical and Biological Engineering.

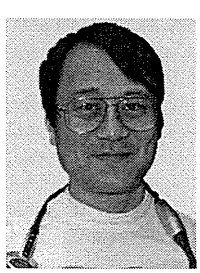

Tomoyuki Yambe received the M.D. and Ph.D. degrees in Medical Science from Tohoku University, Sendai, Japan, in 1986 and 1989, respectively. He was a Research Associate from 1992 at the Division of Medical engineering and Clinical investigation and Department of Medical Engineering and Cardiology, Institute of Development, Aging and Cancer, Tohoku University. He has been a Professor in the some department from 2004. He engages in artificial heart, autonomic nervous system analysis and telemedicine. He is a member of Japanese Society for Artificial Organs, the Japanese Society for Medical and Biological Engineering, and Japanese Society of Neurovegetative Research.